JOURNAL OF MATERIALS SCIENCE 19 (1984) 3149–3158

Diffusion bonds in iron and a low-alloy steel

B. DERBY*, E. R. WALLACH
Department of Metallurgy and Materials Science, University of Cambridge, Pembroke Street, Cambridge, UK

Diffusion bonds made in both the ferrite and austenite iron phases are compared with the predictions of a theoretical model [1, 2]. The initial formation of the bond is shown to be caused chiefly by surface diffusion along interfacial voids. Subsequent void closure occurs by other densifying mechanisms. The model is also used to successfully predict bonding in a low-alloy medium-carbon steel (En8).

1. Introduction

A model of the diffusion-bonding process has been developed [1, 2] as an aid to understanding the mechanisms and kinetics of this fabrication route. The model produces diagrams which show contours of the expected bonded area after given times; it also predicts the dominant bonding mechanism by a conventional mapping technique [3]. To confirm the accuracy of this model, its predictions were compared with a series of experimental bonds fabricated in copper [4]. As a check and to ensure that the results were not peculiar to copper, a further series of bonds were fabricated in iron and a few in a steel (0.4% C). Iron was chosen as a suitable precursor to the study of bonds in steels which would have obvious commercial applications. The data required for the model are all readily available for iron and are listed in Table I.

Iron (and most steels) can exist in two distinct solid phases; the low-temperature ferrite phase (α-iron) with a bcc structure and the higher-temperature austenite phase (γ-iron) with a fcc structure. The phase transition occurs at 910° C (about 0.65 of the melting point) in pure iron. Small additions of carbon as an alloying element lower the transformation temperature to 723° C, above which there exists a two-phase region for a small temperature range. Bonding may be attempted in either of these phases or, in the case of steels, in the two-phase region.

For economic reasons, bonding may be preferred in the lower-temperature ferrite phase because of ever-increasing energy costs. Bonding in the ferrite phase may also have the additional advantage of preserving the microstructure of the steel near the bonded regions; bonds made in the austenite phase would undergo a transformation on cooling. However, the possible bonding mechanisms proposed in earlier work [1, 2] and listed in Table II are mostly temperature-activated and thus faster bonding might be expected in the austenite phase. The two phases have different crystal structures and this too will affect the bonding rates. The lower-temperature ferrite phase has a more open (bcc) crystal structure than that found in austenite (fcc), hence the bcc structure could show faster diffusion at lower temperatures. Bonding in the two-phase region might also be enhanced by the fast diffusion reported along the interphase boundaries [12]. However, since the aim of this work was to compare the model with experimental results, this investigation was confined to single-phase diffusion bonds.

Initially, bonds were made from nominally pure (Remko) iron, an analysis of which is given in Table III. Temperatures were chosen to maintain the materials in either the α- or the γ-phase regions. Preliminary results from the model had indicated that the dominant bonding mechanism would be transfer of material from the free surface of interfacial voids to growing contact necks by surface diffusion. Therefore a study was made of the interfacial void morphologies at various stages of bonding. The void shapes will be dependent on the route of mass transfer adopted

*Present address: Department of Engineering, University of Cambridge, Trumpington Street, Cambridge, UK.

0022–2461/84 $03.00 + .12

TABLE I The data required by the model of diffusion bonding

	α-iron		γ-iron	
Atomic volume (m^3)	1.18×10^{-29}		1.12×10^{-29}	
Burger's vector (m)	2.48×10^{-10}		2.58×10^{-10}	
Melting point (K)	1810		1810	
Density ($kg\,m^{-3}$)	7.87×10^3		7.87×10^3	
Shear modulus ($N\,m^{-2}$)	6.92×10^{10}	[3]	8.1×10^{10}	[3]
Temperature coefficient of shear modulus, $T_M/\mu_0\, d\mu/dT$	−1.31	[3]	−0.91	[3]
Surface energy ($J\,m^{-2}$)	1.95	[5]	1.88	[6]
Volume-diffusion pre-exponent ($m^2\,sec^{-1}$)	2.0×10^{-4}	[7]	1.8×10^{-5}	[7]
Volume-diffusion activation energy (kJ)	239	[7]	270	[7]
Boundary-diffusion pre-exponent ($m^3\,sec^{-1}$)	1.1×10^{-12}	[8]	7.5×10^{-14}	[8]
Boundary-diffusion activation energy (kJ)	174	[8]	159	[8]
Surface-diffusion pre-exponent ($m^3\,sec^{-1}$)	1.6×10^{-8}	[9]	1.1×10^{-10}	[10]
Surface-diffusion activation energy (kJ)	241	[9]	220	[10]
Creep constant	1.4×10^5	[11]	4.3×10^5	[3]
Creep exponent	4.0	[11]	4.5	[3]
Ratio of yield strength to shear modulus	5×10^{-3}		5×10^{-3}	

by the dominant bonding mechanism as listed in Table II [1, 4]. A brief comparison of the model's predictions with bonds in En8 (0.4% C) steel was also made.

2. The model

The model is described fully in previous work of the authors [1, 2] and a brief resumé presented in a previous article in this publication [4]. Therefore only an outline will be given here. Diffusion bonding is assumed to occur when the two faying surfaces achieve intimate contact across the bonding interface. Normal surfaces are held apart by their roughnesses. The rate-determining process has therefore been modelled as the deformation of this roughness to produce a partly bonded morphology of long voids. A complete bond occurs when this interface porosity has been removed.

Diffusion bonding is dependent on a combination of microdeformation and diffusion mechanisms operating at the interface, some of which are indicated in Table II. By considering the action of each of these mechanisms on a representative surface, a simple iterative model was derived. The important process parameters were revealed to be temperature, bonding load and surface roughess. The results of the model and its dependence on these parameters were displayed by a conventional mapping technique [3], which also indicated which mechanism had the greatest contribution to the rate as bonding progressed.

3. Comparison of bonds with the model's predictions

The bonding procedure was as follows. The specimens to be bonded were cut to length from 12.5 mm diameter rod, the ends to be bonded were ground flat and degreased prior to insertion into the bonder. The mean surface roughness was approximately 0.5 μm peak-to-valley height, with a mean surface wavelength of 50 μm. The bonder was evacuated to 10^{-3} Pa, the surfaces were brought into contact at the bonding pressure and then heated to the bonding temperature by a ratio-frequency (r.f.) induction furnace. Time to reach bonding temperature was typically about 1 min. After the required bonding time had

TABLE II Some possible diffusion-bonding mechanisms

Mechanism	Effect
1. Plastic deformation	instantaneous deformation of surface asperities or collapse of interfacial voids
2. Creep flow	deformation of surface asperities or collapse of interfacial voids
3. Surface diffusion	transfer of material from void surface to a growing neck; increased bond area, pore volume unaffected
4. Grain-boundary diffusion (along bond interface)	transfer of material from within the specimens to a growing neck; increased bond area, decreased pore volume
5. Bulk diffusion	combination of 3 and 4 but, in general, much slower

TABLE III Composition of the iron used in the bonding experiments

Impurity	Concentration (wt %)
C	0.003
P	0.004
S	0.004
Si	0.001
Mn	0.002
Cu	0.006
Sn	0.006
As	0.002
Zn	0.001
Pb	0.002
Al	0.005
Ni	0.003
Co	0.002
Zr	0.002
Mo	0.002
V	0.002
Ge	0.001
Cr	0.004
Cl	trace
O	0.032
H	0.002
N	0.002
Ti	0.001

elapsed, the specimens were unloaded and cooled by filling the chamber with argon. Throughout the bonding cycle, the bonding pressure was monitored and adjusted to maintain a constant value. On removal from the bonder, the bonds were sectioned and examined with a light microscope to determine the extent of bonding. This bond-assessment method was not ideal and tended to produce a significant scatter of results from the same specimen. The sections were also examined with a scanning electron microscope (SEM) in order to examine the interface-void morphology.

3.1. Diffusion bonds in α-iron

Bonds were made in Remko iron at 700 and 850° C using bonding pressures of 5 MPa, 7 MPa and 15 MPa. Fig. 1 shows the predicted temperature-dependence of bonding: superimposed are the measured bonded areas determined from experimental bonds. Fig. 2 shows the same for the pressure dependence of bonding. The agreement between experiment and the model's predictions are good, apart from the specimen bonded at 850° C. Fig. 3 indicates the predicted extent of bonding as a function of time and again a reasonable fit with experiment is seen. From the mechanism maps (Figs. 1 and 2), the dominant bonding mechanism is expected to be surface diffusion at low bonding-pressures while above about 12 MPa power-law creep is expected to become important.

3.2. Diffusion bonds in γ-iron

Bonds were made at 1000 and 1100° C to test the model in the γ-phase. A bonding pressure of

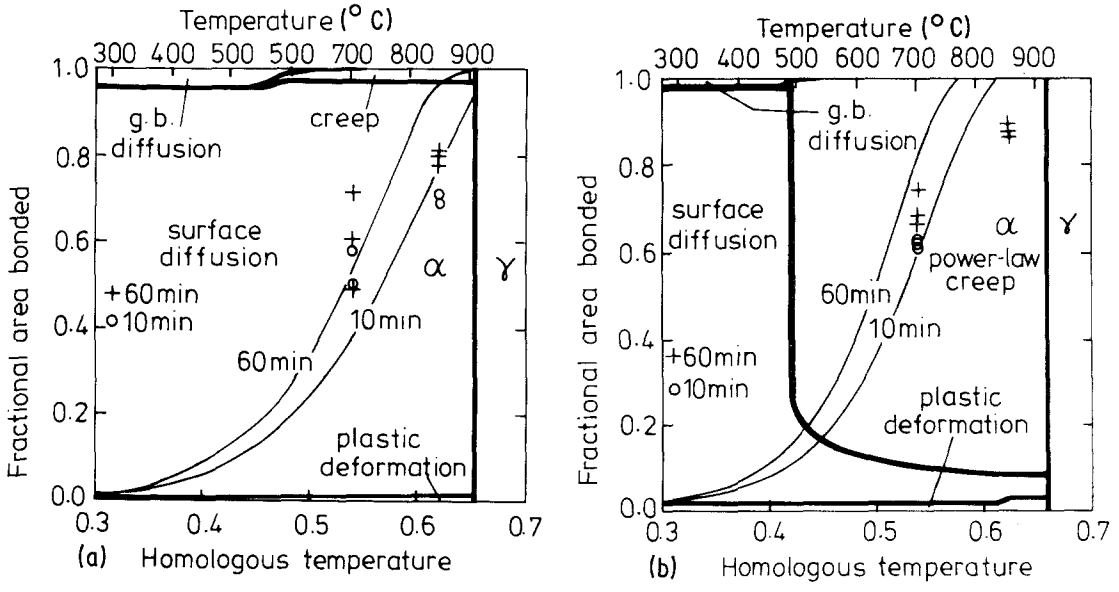

Figure 1 Comparison of experiment (points) with the model's prediction for the variation of diffusion-bonding time in α-iron with temperature (contours of 10 and 60 min). Bonds were fabricated in Remko iron of roughness height 0.6 μm and wavelength 55 μm for times of 10 and 60 min at applied pressures of (a) 7 MPa, (b) 15 MPa.

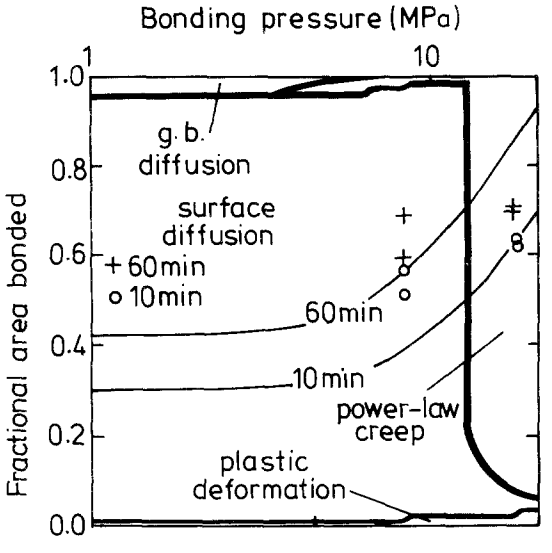

Figure 2 Comparison of experiment (points) with the model's prediction for the variation of diffusion-bonding time in α-iron with applied pressure (contours of 10 and 60 min). Bonds were fabricated in Remko iron of roughness height 0.6 μm and wavelength 55 μm for 10 and 60 min at a temperature of 700° C.

7 MPa was used because at higher pressures a large-scale distortion of the specimens occurred. This deformation was found to occur away from and on either side of the bonding interface. The r.f. induction furnace heats a very narrow zone around the bond and the temperature falls away rapidly from this hot zone. It is believed that the barrelling distortion observed away from and on either side of the bond is caused by creep in the α-phase just below the transition temperature. The effect has not been observed in steels, possibly because a two-phase structure exists on either side of the hot zone. In such a structure, there will not be large amounts of ferrite at high temperatures because of the increasing fraction of austenite at high temperatures.

Fig. 4 compares the predicted temperature variation in bonding with that found experimentally. The agreement with the model is exceptionally good. As with the bonds in α-iron, the expected dominant bonding mechanism is seen to be surface diffusion.

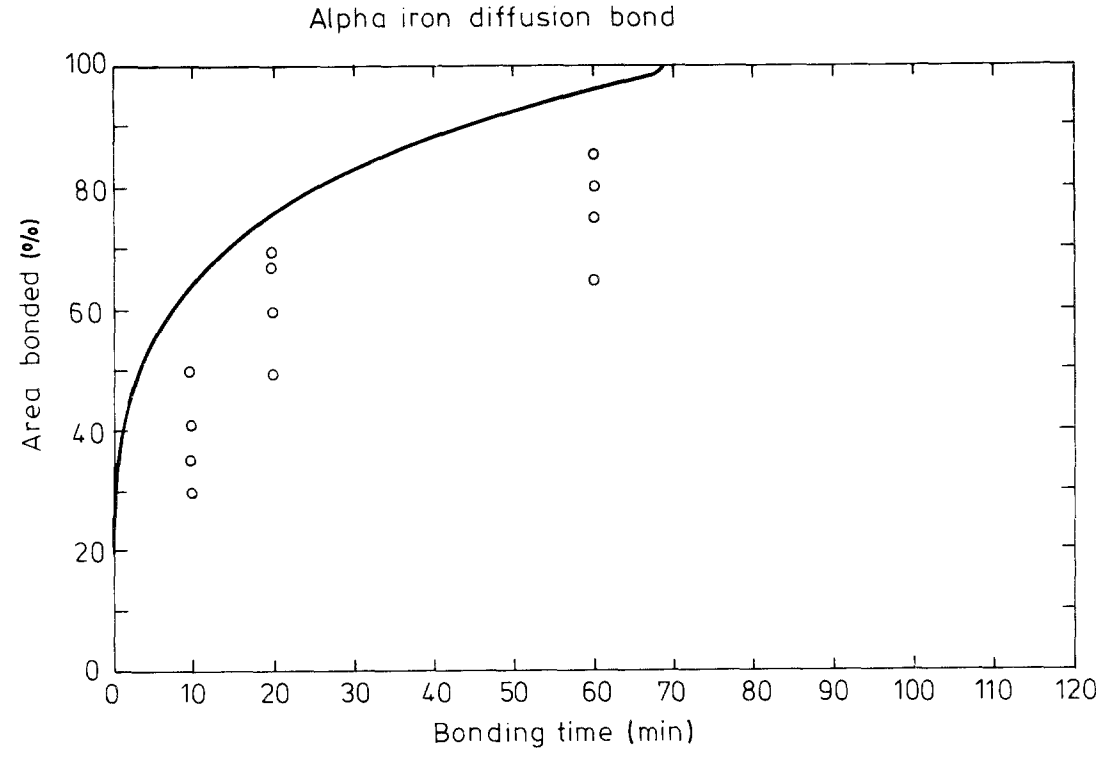

Figure 3 The progress of diffusion bonding in α-iron. Experimental results are shown as points and the prediction of the model is the continuous line. Bonding conditions were: temperature 700° C, applied pressure 4 MPa, surface-roughness height 0.4 μm and wavelength 50 μm.

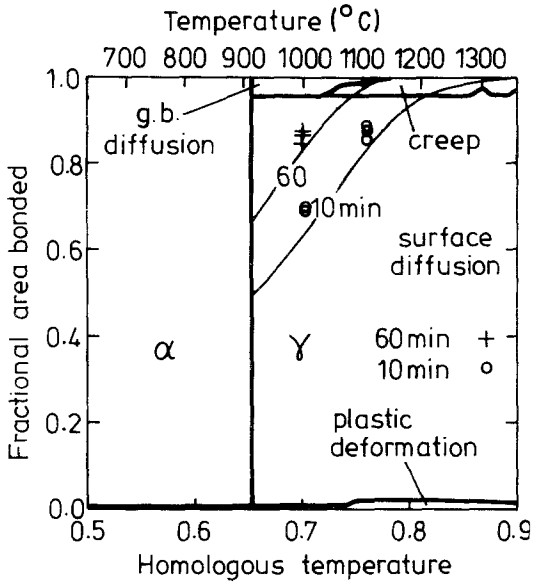

Figure 4 Comparison of experiment (points) with the model's prediction for the variation of diffusion-bonding time in γ-iron with temperature (contours of 10 and 60 min). Bonds were fabricated in Remko iron of roughness height 0.6 μm and wavelength 55 μm for times of 10 and 60 min at an applied pressure of 7 MPa.

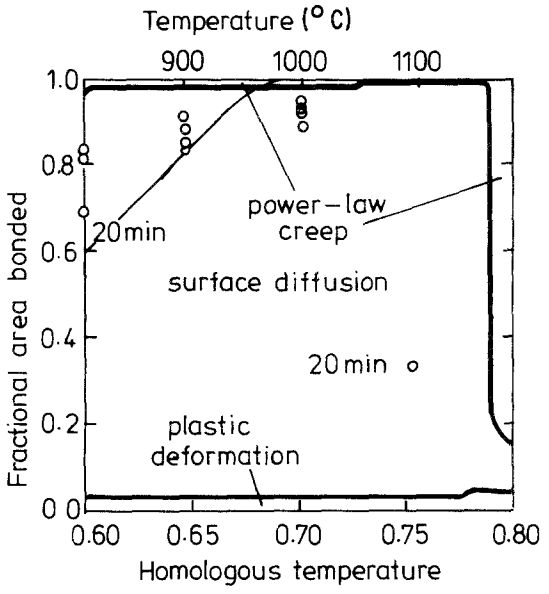

Figure 5 Comparison of experiment (points) with the model's prediction for the variation of diffusion-bonding time in a low-alloy steel with temperature (contours of 10 and 60 min). Bonds were fabricated in En8 steel of roughness height 0.4 μm and wavelength 50 μm for times of 10 and 60 min at an applied pressure of 7 MPa.

3.3. Diffusion bonds in En8 steel (0.4% C)

Diffusion is predominantly a lattice property. In iron, it is found that small additions of alloying elements in solution (e.g. carbon, nickel, manganese or chromium) do not greatly affect the activation energies or coefficients of diffusion [13]. The work of Brown and Ashby [14] correlated the diffusion properties of metals to their crystal structures and melting temperatures, which in steels do not change to a great degree on slight alloying. Creep coefficients, however, show a much greater variation because of the influence of microstructure and lattice strains on dislocation behaviour. Thus, in general, steels are expected to be much more creep-resistant than pure iron. For the iron specimens bonded at lower stresses, it was found that creep did not play an important part. Therefore, if no information was available on the creep behaviour of a steel, the effect of possible changed creep data (which would render creep even more difficult) was ignored in the model. Bonds were only made in the higher-temperature γ-phase because at lower temperatures a cementite phase would be present with the ferrite, hence complicating analyses of the bonding mechanisms.

Some bonds were made in En8 steel (0.4% C and 0.65% Mn) in the γ-phase. The data for creep and diffusion in austenite of this alloy composition was not known but work on the deformation of similar composition alloys in the γ-phase [3] has indicated a similarity to the behaviour of pure austenite, and so the data of pure austenite was used. The bonds were made at a uniform pressure of 20 MPa with the same surface roughnesses as were used for the iron bonds. The process was halted after 20 min and the extent of bonding determined. The measured extent of bonding is shown with the predictions of the model in Fig. 5; again, good agreement between model and experiment is found. As with the bonds made in the pure iron specimens, the dominant bonding mechanism is predicted to be surface diffusion.

4. The bonded interface in iron

From the figures shown in the previous section, it can be seen that the predicted dominant bonding mechanism for most ferrous alloys under typical bonding conditions is surface diffusion. To confirm this, partly bonded specimens were examined to see if the observed interfacial void shapes agreed

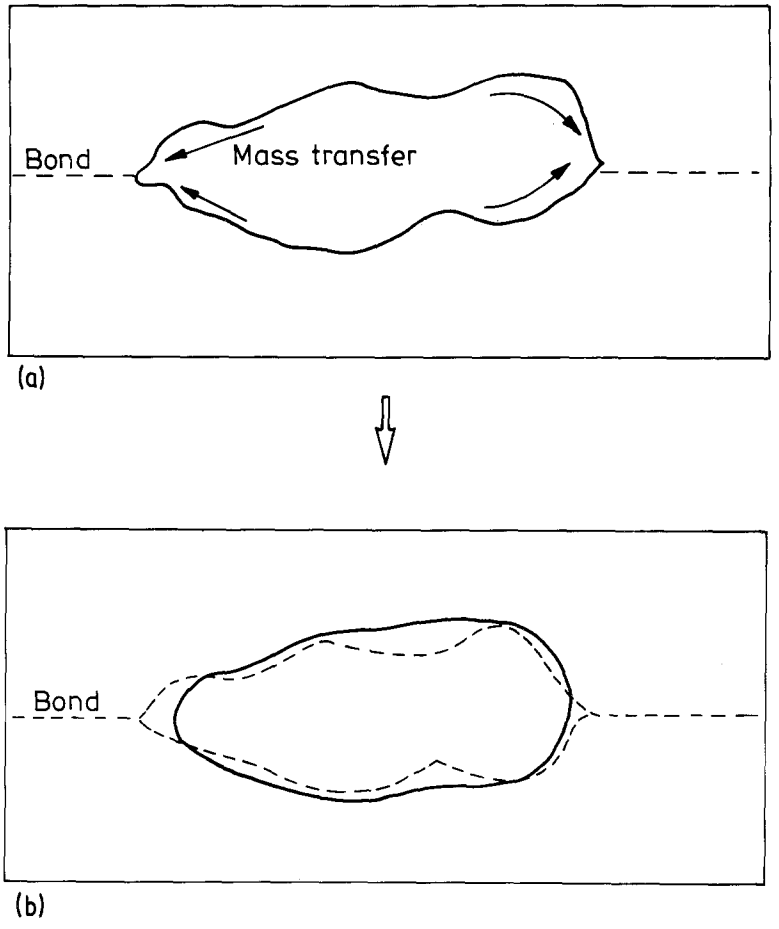

Figure 6 The influence of the surface diffusion-bonding mechanism on void shape. The material is transferred to regions of high surface-curvature, thus smoothing out the shape. The net result is to diminish the void width while increasing its height, volume remaining constant.

with those expected from the action of surface diffusion. This is feasible because each bonding mechanism alters the interface morphology in a characteristic manner [1, 4]. Surface diffusion transfers material from the void surfaces to the interface; at the start of bonding, localized yield at the points of initial surface contact will create voids with sharp corners at the bonded interface (Fig. 6a). When surface diffusion operates, these sharp necks will be rounded off (Fig. 6b) because the mechanism driving force (the Joule–Thompson effect) transfers material to regions of high surface-curvature. Surface diffusion does not alter the volume of the interfacial voids [1], but the redistribution of matter changes their shape to a more circular profile while also increasing the bonded area. If bonding is to be achieved then other bonding mechanisms must operate in concert with surface diffusion to eliminate this interface porosity, and so at some stage in the process these other mechanisms will affect the interfacial morphology. However, because of the predicted dominance of surface diffusion, it was assumed that at least in the early stages of bonding (when there is clear surface-diffusion dominance) voids similar to those in Fig. 6 would be seen.

Interfacial voids present in a diffusion bond fabricated for 10 min at 700° C with 7 MPa pressure are shown in Fig. 7. The voids are clearly rounded, indicating the dominance of diffusional mechanisms. The voids are quite large, with a height of about 2 μm. The measured peak-to-valley surface-roughness height prior to bonding is about 0.5 μm (accurately assessed as 0.6 μm by surface profilometry), and so void heights are expected to be about 1 μm at the start of bonding. The bond in Fig. 7 has a measured bonded area of about 50% but the interfacial void is seen to be higher (2 μm) than that expected with zero bonded area (1 μm). Surface diffusion is expected to transfer material from the void surfaces to a neck on the bonding interface (Fig. 6); this will have the effect of increasing the void height as bonding proceeds. Therefore the observed increase

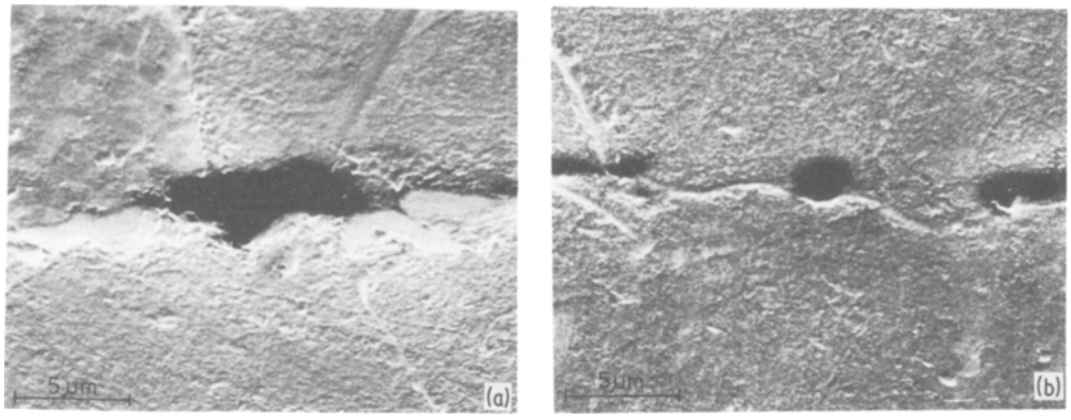

Figure 7 SEM micrographs of interfacial voids in α-iron after 10 min bonding at 700° C and 7 MPa.

in void height in Fig. 7 is taken as important evidence for the operation of surface diffusion.

Interfacial voids present in specimens bonded for 10 min at 1000° C with 7 MPa pressure in the γ-phase are shown in Fig. 8. These voids again are rounded and higher than expected. Even after 60 min bonding, when the bonded area is expected to be in excess of 80%, void heights greater than a micrometre are found (Fig. 9). Note also how the voids in the γ-iron bonds appear to have split into packets of smaller voids: this was also observed in some of the α-iron bonds (Fig. 7b). A similar void-packet interface structure has been reported in low-alloy-steel diffusion bonds [15].

5. Discussion

The agreement between the previously derived model [1, 2] and the experimental results presented here is good. A small error is apparent in that the model consistently predicts slightly better bonding than is found, especially at longer bonding times. It is possible that, in the final stages of bonding, there may be retardation forces not taken into account in the model, e.g. entrapped gas in the voids or possibly tenacious surface contaminants. The rather worse agreement seen in Fig. 1 may have been caused by poor temperature control allowing the specimen to drift into the γ-phase field during bonding. Such a temperature drift may explain the interface morphology shown in Fig. 10, where the interfacial grain-boundary is seen to have migrated away from the interfacial voids. If a diffusion bond is made in a single-phase material, no grain growth occurs across the interface, usually because of pinning by segregated impurities. Therefore this would indicate that the bond made nominally at 850° C may have been made in the

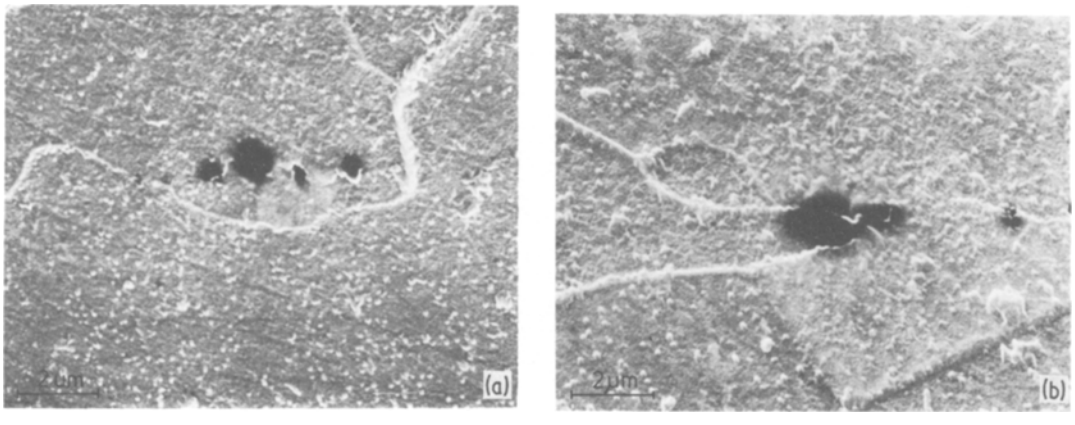

Figure 8 SEM micrographs of interfacial voids in γ-iron after 10 min bonding at 1000° C and 7 MPa: (a) void packet, (b) void split into two.

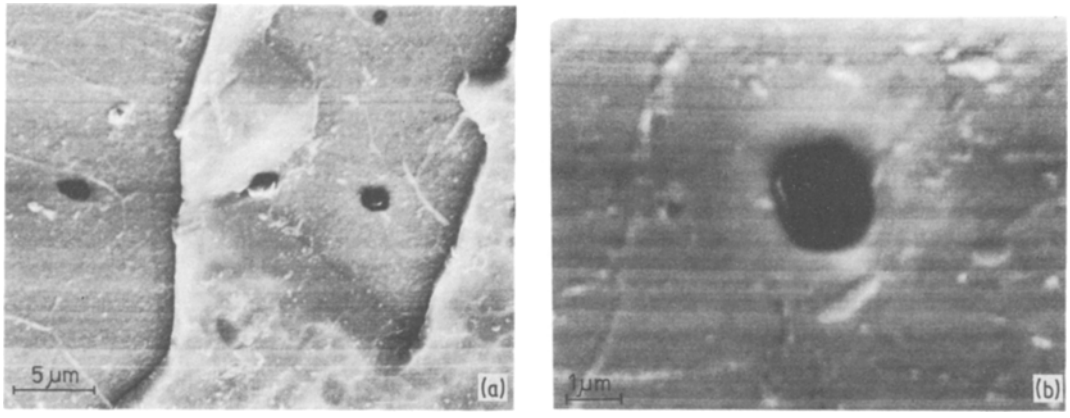

Figure 9 SEM micrographs of interfacial voids in γ-iron after 60 min bonding at 1000° C and 7 MPa: (a) several voids, (b) single large void.

γ-phase at a slightly higher temperature and the observed boundary migration would then be a result of the phase change on cooling.

Apart from the above, the most likely reason for the general slight disagreement between the model and reality is the modelling of surface roughness. The surface used in the bonding model is taken as being a simple array of long, triangular ridges. Although this is probably an accurate enough model for surfaces prepared for bonding by lathing, it certainly does not describe a surface prepared by grinding (Fig. 11). Such a ground surface can be thought of as comprising two surface roughnesses with differing superimposed wavelengths [16]. On bonding, it is possible that the subsidiary wavelength might touch and form a second void; this could subsequently lead to a complete splitting of the void into a packet of smaller voids (see Fig. 12). Such a void-packet morphology is perhaps seen in Fig. 8.

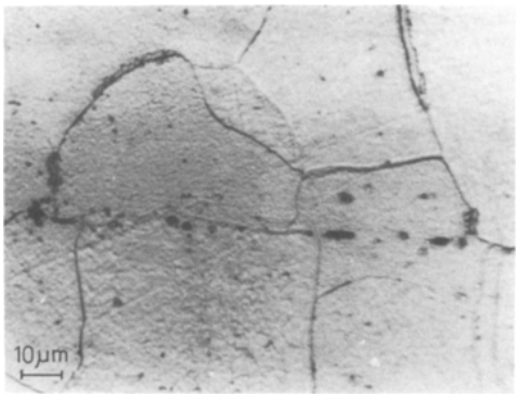

Figure 10 Light micrograph of the bonding interface in α-iron: the interfacial grain boundary appears to have migrated away from the voids. Bonded for 10 min at 850° C and 7 MPa with a surface roughness height of 0.6 μm and wavelength 60 μm.

It is important to consider whether or not a packet of voids can form because the effect of such a morphology on the driving force for diffusion bonding might be significant. Surface diffusion, for example, transfers material from regions of low surface-curvature to those of high curvature within one void. The void packet of Fig. 12 results in one elongated void being replaced by several voids, none of which can support bonding by surface diffusion because of their circular section, and so the bonding rate would be affected. However, the overall effect of a packet morphology is more complex than assuming a simple reduction in the bonding rate. As each void contributes a normal tension across the interface by virtue of the solid–void surface energy, a proliferation of voids will increase the normal load on the interface and so accelerate some other bonding mechanisms.

6. Conclusions

The dominant mechanism for diffusion-bonding iron and steels has been shown to be initially surface diffusion, although other mechanisms result in final void closure. This emphasizes the importance of the preparation of the surface state prior to bonding. Although grinding produces a fairly low surface roughness which is expected to aid bonding [1], it also creates a void-packet morphology which may be detrimental to the removal of all residual porosity.

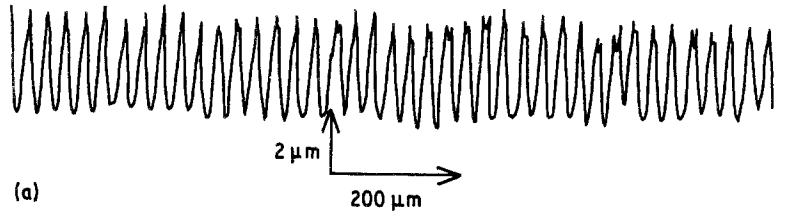

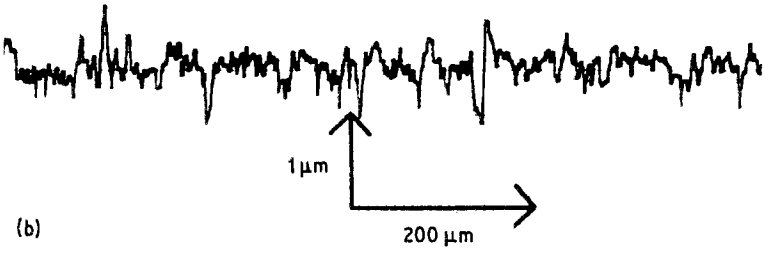

Figure 11 Roughness traces of surfaces prepared for bonding by (a) lathing, (b) grinding.

In terms of the model, a very encouraging agreement between prediction and result is found. Despite the lack of specific information, it seems to be possible to model low-alloy steels in the γ-phase using the data of pure iron, probably because of the dominance of diffusional mass-transport bonding mechanisms, which are not expected to be very sensitive to small alloy-additions. At lower temperatures in the α-phase, the effect of creep may not be small and it will be necessary to find data to model this. However, creep data are more plentiful than diffusion data and it should easily be possible to determine the appropriate model parameters using the creep-constitutive equation.

Acknowledgements

The authors would like to thank Professor R. W. K. Honeycombe for the provision of laboratory space and the Science and Engineering Research Council for financial support. We would like to thank C. E. Thornton who fabricated the bonds in En8 steel.

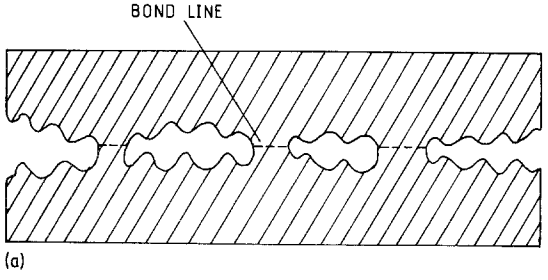

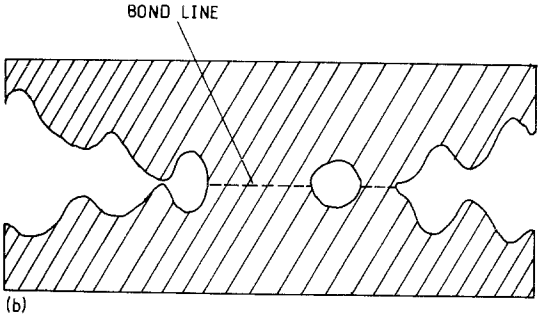

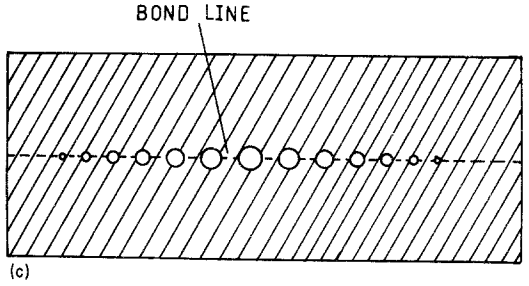

Figure 12 Possible effect of the secondary roughness on interfacial-void shape. (a) Initial stages of bonding leading to primary contact. (b) Possible second contact ahead of primary neck. (c) Eventual multiple contact and subsequent void splitting leading to a packet of smaller voids.

References

1. B. DERBY and E. R. WALLACH, *Metal. Sci.* **16** (1982) 49.
2. *Idem, ibid.* (In press.)
3. H. J. FROST and M. F. ASHBY, "Deformation Mechanism Maps" (Pergamon, Oxford, 1982).
4. B. DERBY and E. R. WALLACH, *J. Mater. Sci.* **19** (1984) 3140.
5. H. JONES, *Metal Sci.* **5** (1971) 15.
6. L. E. MURR, "Interfacial Phenomenon in Metals and Alloys" (Addison Wesley, Reading, Mass, 1975).
7. F. S. BUFFINGTON, K. HIRAWO and M. COHEN, *Acta Metall.* **9** (1961) 434.
8. D. W. JAMES and G. M. LEAKE, *Phil. Mag.* **12** (1965) 491.
9. J. M. BLAKELY and J. MYKURA, *Acta Metall.* **10** (1962) 565.
10. G. NEUMANN and G. M. NEUMANN, "Surface Self Diffusion of Metals" (Diffusion Information Centre, Bay Village, Ohio, 1972).
11. R. D. CALIGURI, PhD thesis, Stanford (1977).
12. J. JUVE-DUC, D. TREHEUX and P. GUIDRALDENQ, *Mater. Sci. Eng.* **42** (1980) 281.
13. J. ASKILL, "Tracer Diffusion Data for Metals, Alloys and Simple Oxides" (Plenum, New York, 1970).
14. A. M. BROWN and M. F. ASHBY, *Acta Metall.* **28** (1980) 1085.
15. C. E. THORNTON, "Diffusion Bonds in Steel", PhD thesis, Cambridge (1983).
16. S. E. ELLIOT, E. R. WALLACH and I. A. BUCKLOW, *J. Mater. Sci.* **15** (1980) 2823.

Received 30 September
and accepted 11 October 1983